Matrix Isolation and Density Functional Theory Study of Bis(trifluoromethyl)dioxodiazine: A Photodimer of Trifluoronitrosomethane

Brendan C. Haynie,[†] Megan J. Morgan,[‡] and Christopher A. Baumann*

Department of Chemistry, University of Scranton, Scranton, Pennsylvania 18510-4626

Received: February 10, 2005; In Final Form: April 19, 2005

Trifluoronitrosomethane (CF_3NO) was trapped in rare gas matrixes and irradiated at 633 and 670 nm. The infrared spectra of the postirradiation samples exhibit features consistent with *cis* and *trans* conformers of bis(trifluoromethyl)dioxodiazine, a previously uncharacterized species. The concentration dependence of the formation of the dimer is consistent with a mechanism in which monomers trapped in adjacent sites undergo excitation and subsequent reaction. The dimers reversibly form the monomer when irradiated with ultraviolet light. Density functional theory was used to determine the structure of the dimers and predict their infrared and Raman spectra. The predicted vibrational frequencies are in agreement with those observed. A third (skewed) conformation was predicted to have a triplet ground state, but no evidence of this species was observed. All three dimers exhibit significant diradical character, as evidenced by comparatively low N−N and high N−O stretching frequencies. Transition-state calculations predict the dimerization barrier to range from 17.1 (*cis*) to 35.0 (*trans*) kJ mol^{-1} for the singlet dimers and to be 62.1 kJ mol^{-1} for the triplet dimer. This is an example of nitroso dimerization that *requires* electronic excitation to proceed.

Introduction

The dimerization of *C*-nitroso compounds has been studied for over 100 years.[1] Most of the *C*-nitroso compounds that dimerize form diazene dioxide products, the result of NN connection of the monomeric species.[2] Attempts to form the traditional dimer from trifluoronitrosomethane (CF_3NO) have not been successful,[3−7] yielding instead *O*-nitrosobis(trifluoromethyl)hydroxylamine ($(CF_3)_2NONO$). Recent kinetic studies of the photolysis of CF_3NO have also shown this to be the case:[8] photolytically produced CF_3 radicals react with nearby CF_3NO molecules, and the resulting $(CF_3)_2NO$ reacts with NO. The instability of the diazene dioxide $(CF_3NO)_2$ dimer has been attributed to the electron-withdrawing ability of the trifluoromethyl moiety.[2,9]

The matrix-isolated CF_3NO molecule has been studied via a variety of spectroscopic techniques. Goodman and Brus observed the excitation and emission spectra of the molecule trapped in a nitrogen matrix, attributing a broad emission to dimeric and polymeric species with radiative lifetimes of 257 and 78 ns, respectively, compared to the 344 ns monomer lifetime (285 ns in neon).[10] Bozlee and Nibler followed the excited-state relaxation using fluorescence and photoacoustic spectroscopy.[11] The infrared spectrum of the molecule in matrixes was obtained by Demuth and co-workers,[12] and later by Clemitshaw and Sodeau.[13] These were in agreement with the gas-phase spectra observed by Mason and Dunderdale[14] and later by Shurvell and co-workers.[15] The infrared studies yielded no evidence of dimers or higher polymers in matrixes, but the condensed-phase Raman studies performed by Shurvell et al. resulted in source-produced peaks that could not be assigned to the monomer. Irradiation of the dilute matrixes leads to the production of proximity radicals, where the photolytically produced CF_3 is perturbed by neighboring intact molecules.[13]

Recent work in this group includes laser irradiation of CF_3NO adsorbed on thin films of condensed inert gases, which was conducted as a followup to attempted laser photolysis on alkali-metal halide surfaces.[16] The overlayer studies indicated the presence of a photoproduct produced as a result of laser ($\lambda = 633$ and 670 nm) irradiation of CF_3NO, whereas the alkali-metal halide surfaces completely quenched S_1 photochemistry in the molecule. The photoproduct did not possess the same characteristics of the *N*-nitritoamine reported by Mason.[6,7] To characterize the photoproduct, a series of matrix isolation experiments were performed. In this paper we report the results of visible laser irradiation of CF_3NO in the condensed phase at low temperatures; the reaction progress was monitored through infrared spectroscopy. The infrared spectrum and observed apparent quantum efficiencies are consistent with the formation of dioxodiazine dimers, and agree with the vibrational spectra predicted by density functional calculations. This is the first example of a nitroso compound found to dimerize *exclusively* via electronic excitation.

Experimental Section

The equipment for these experiments has been described in a previous paper.[16] The CF_3NO for these experiments was obtained from SCM Corp. Specialty Chemicals, Gainesville, FL. A trifluoronitromethane impurity (∼5%) was noted by the manufacturer, and observed in the infrared spectra. The argon, oxygen, and nitrogen were JWS Technologies PP grade gases. The krypton and xenon were research grade (listed as 99.998% pure) and were obtained from Matheson Gas Products. All gases were used without any further purification. The mixing ratios were determined using standard manometric procedures.

Each individual matrix mixture (consisting of CF_3NO in Kr, Xe, Ar, N_2, or O_2) was introduced into the system via a filling

* To whom correspondence should be addressed. E-mail: CAB302@scranton.edu.

[†] Current address: School of Arts and Sciences, Kentucky Christian University, Grayson, KY 41143.

[‡] Current address: Titleist and Foot-Joy Worldwide, P.O. Box 965, Fairhaven, MA 02719-0965.

10.1021/jp050730z CCC: $30.25
Published on Web 05/26/2005

line. The gas mixture was introduced into the cryostat through a thin nickel inlet tube, which allowed the gas to be projected directly onto the internal KBr window when the shroud is situated such that the window is facing the inlet. The geometry of the windows around the inlet allowed irradiation during deposition, either through the internal window (irradiating the matrix as well as the incoming gas) or between the window and the inlet tube (without irradiating the matrix). The system base pressure was $\sim 1 \times 10^{-6}$ Torr.

All infrared spectra (32 or 100 coadded scans at 1 cm^{-1} resolution) were obtained on a Mattson Galaxy 5022 Fourier transform infrared spectrometer with a DTGS detector. A background spectrum (32 or 100 coadded scans at 1 cm^{-1} resolution) was acquired at a temperature of 20 K prior to deposition of the matrix. Matrixes were deposited at 20 K and the flow was adjusted to maintain a pressure range of $(0.4-2.0) \times 10^{-5}$ Torr. Spectra were acquired immediately following deposition, as well as before and after each photolysis increment.

Once the matrix had been deposited, irradiation was performed. The samples were irradiated with light from a Uniphase 1335 10 mW helium/neon laser (633 nm) or an Imatronic LDL 175 3 mW diode laser (670 nm). The low laser power will minimize the degree to which multiphoton processes occur. UV irradiation was provided by the unfiltered output of a Beckman, Inc. 71701 deuterium lamp. Laser power was determined with a Metrologic 45-540 power meter, calibrated for use at 633 nm. The initial experimental temperature was set at 12 K. The temperature was then increased over the course of each procedure in 6 K increments. Thus, at each temperature, an initial spectrum was obtained; irradiation occurred for 60−120 min, another spectrum was obtained, and the temperature was reset to a higher temperature until the particular matrix showed signs of instability. The high concentration of solute in some of these matrixes led to deviations from the expected matrix degradation temperatures (roughly half of the normal melting point temperature of the pure matrix gas).[17]

For each matrix gas there were several experiments conducted at various concentrations. The concentrations (CF_3NO:RG) for the Ar matrix were 1:30, 1:73, 1:530, and 1:4000, those for O_2 were 1:62 and 1:470, those for Kr were 1:41, 1:400, and 1:2800, those for N_2 were 1:57, 1:392, and 1:1900, and that for Xe was 1:49. For one of the concentrated argon matrix experiments and the xenon matrix experiment, the sample was kept in the dark for periods of several hours to determine the stability of the photoproducts at these temperatures.

Results

Infrared Spectra and Photochemistry. The spectrum of matrix-isolated CF_3NO was in agreement with the gas-phase[14,15] and matrix[12,13] values reported elsewhere. There is very little variation of peak shape and position from experiment to experiment, although some broadening is observed in matrixes having dilution ratios of less than 1:100.

Upon visible irradiation, new peaks are observed and the original CF_3NO peaks exhibit reduced absorption. Figure 1 shows the results (as a difference spectrum) of irradiation at 633 nm. The preirradiation spectrum was subtracted from the postirradiation spectrum, giving a resultant spectrum indicating any gains in the spectrum as a result of photolysis as positive peaks and losses as negative peaks. The parent species lost during photolysis will exhibit negative peaks, while the product species will exhibit positive peaks. Table 1 is a cumulative list of the observed postirradiation peaks. The matrix material has little effect on the vibrational frequencies of the photoproduct.

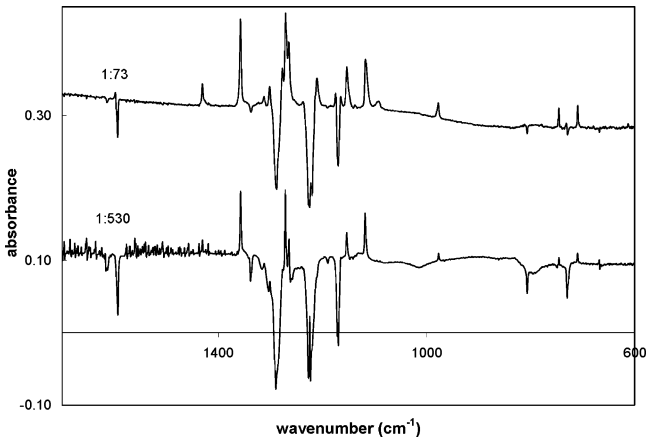

Figure 1. Difference spectra for CF_3NO in argon at dilutions (R:M) of 1:73 and 1:530. These spectra are the result of subtracting the preirradiation spectrum from postirradiation spectra (633 nm at 20−24 K for 2 h). Positive peaks correspond to photolytic products; negative peaks correspond to species lost as a result of irradiation.

TABLE 1: Peaks (Frequencies, cm^{-1}) Observed after Visible Irradiation of Matrix-Isolated CF_3NO

argon	krypton	xenon	nitrogen	oxygen
	2846		2853	2858
1431			1431	1429
	1426	1427	1427	
1357	1357	1354	1359	1358
1302			1316	
1271	1267	1265	1267	1268
1209				
1165				
1153	1145	1146	1150	1148
1117	1112	1111	1114	1112
1095	1091	1090	1094	1092
977	982	976	980	981
		779		
				750
746	746	745	747	747
709	709	709	709	709

The peaks grow in proportionately, indicating that they belong to a single (or multiple, but stoichiometrically related) species. The CF_3NO_2 impurity shows little variation under visible irradiation.

We do not observe spectra characteristic of $(CF_3)_2NONO$, nor do we observe products of the fragmentation of the parent compound. Annealing or UV irradiation did not change any of the photoproduct peaks differently from the others. Since the IR spectrum of the photoproduct did not resemble that of the $(CF_3)_2NONO$ isolated by Mason,[6,7] we sought other possible structures to account for the spectral features. The complete lack of observable fragmentation products such as NO, CF_3, $(CF_3)_2NO$, or $(CF_3)_2NONO$ led us to conclude that the product does not arise from photolytic cleavage of the C−N bond in the parent compound. Visible irradiation directly above the window surface during deposition, which would result in excitation of the CF_3NO in flight immediately prior to condensation, did not yield observable levels of product.

Figure 2 shows the rate with which the integrated absorbances of the peak at 1357 cm^{-1} varies with the matrix dilution, normalized for initial parent population and laser power. The increase in the absorbance of the photoproduct peak at 1357 cm^{-1} was divided by the duration of irradiation, and the amount of incoming 633 nm radiation absorbed by the parent (based on the preirradiation height of the 1595 cm^{-1} peak). All measurements depicted were made between 12 and 14 K. The line in the figure depicts the maximum observed rate (for all

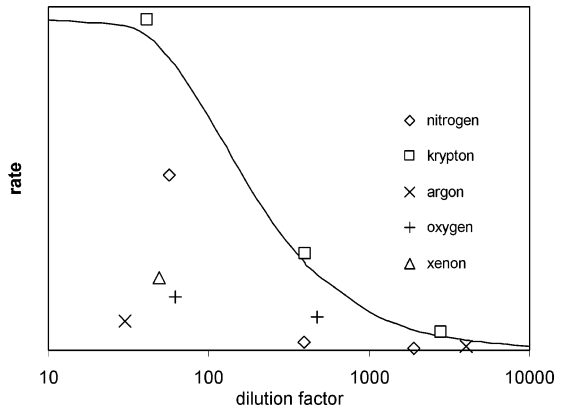

Figure 2. Rate of initial photoproduct production at 633 nm as a function of CF_3NO dilution.

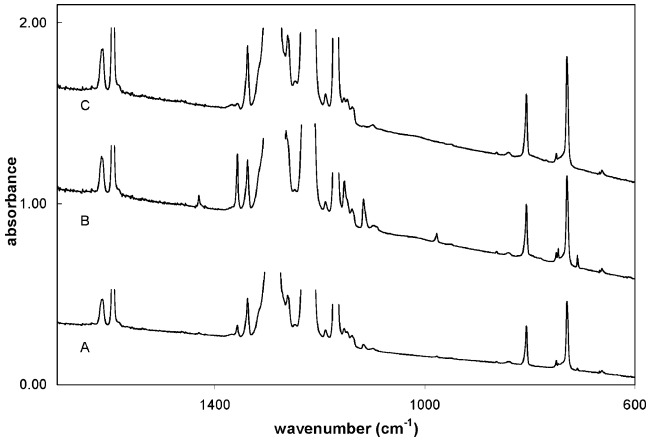

Figure 3. UV depletion of photoproducts in an argon matrix (CF_3NO:M = 1:73). Spectrum A was acquired after irradiation during matrix deposition. Spectrum B was acquired after 120 min of 633 nm irradiation at 24 K. Spectrum C was acquired after 88 min of UV irradiation at 12 K.

matrixes in this study) attenuated by the probability of another monomer molecule inhabiting an adjacent site. It is clear from Figure 2 that the product is formed more readily in concentrated matrixes. At the highest dilutions, approaching true matrix isolation conditions, the photoproduct levels are barely discernible. The concentration dependence indicates that the product arises from interactions between adjacent parent molecules. It is also apparent that the rate of production is not significantly slower in an O_2 matrix than in another matrix of comparable dilution. The effect of laser flux on dimer production is approximately linear.

After visible irradiation, the system was irradiated with unfiltered ultraviolet light for times ranging from 30 to 90 min. The result of the process is the visible product species disappeared, indicated by the loss of all corresponding absorbances in the IR spectra, and upon this destruction, no new absorbances were observed. Figure 3 shows the results of one such irradiation sequence (preirradiation, after visible irradiation, and after UV irradiation). It is important to note that no new species are observed as the result of UV irradiation of a matrix containing the visible photoproduct. In this figure, the tops of the peaks belonging to the parent species were chopped for scale purposes.

The stability of the visible photoproduct was monitored by observing the spectrum over time at several temperatures. As noted previously, the cryostat was kept in the dark throughout this period: the entire apparatus was shrouded with black cloth in a darkened room, and the IR beam was blocked to avoid

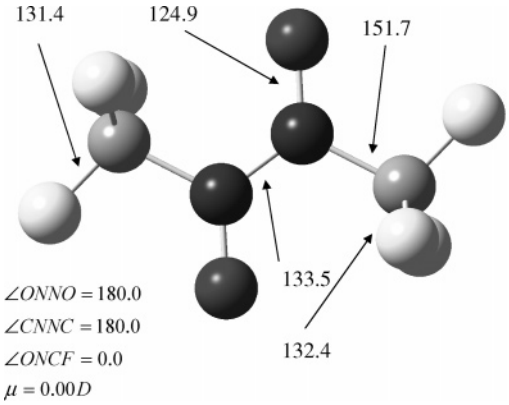

Figure 4. DFT structure of *trans*-bis(trifluoromethyl)dioxodiazine. Distances are given in picometers.

stray visible or NIR light from the source or the alignment laser. Under these conditions, all photoproduct peaks retained their absorbances over a period exceeding 10 h. When the xenon matrix was warmed above 40 K, some gradual loss was noted, but this was accompanied by a comparable loss of the parent peaks, indicating the degradation of the matrix. The visible photoproduct appears to be a stable species, and not a transient intermediate.

The infrared spectrum of the monomer in our previous studies[16] on the surfaces of condensed rare gases and in overlayers on alkali-metal halide films is identical to that of the "glassy liquid" phase observed by Shurvell and co-workers.[15] The infrared spectrum of the matrix photoproduct is nearly identical to that of the surface photoproduct above. Thus, we may infer that the source-induced peaks Shurvell et al. observed growing into their Raman spectra belong to the same species that is observed in our infrared spectra. The most prominent of the source-induced peaks observed by Shurvell et al.[15] in the Raman spectrum of the glassy liquid was located at 1515 cm^{-1}. Since we see no evidence of a peak at 1515 cm^{-1}, we assume that it belongs to a centrosymmetric photoproduct and, given its frequency, attribute it to a symmetric N═N or N═O stretch. Shurvell et al. also observed other unassigned peaks in the Raman spectra at 1122, 334, and 134 cm^{-1}, but these were all much weaker than the very intense 1515 cm^{-1} peak.

Density Functional Theory. *Dimers.* The above led us to consider the possibility that the photoproducts are the *cis* and *trans* conformers of a dioxodiazine, the structure exhibited by many *C*-nitroso dimers; thus, we fit the spectrum to that for *cis*- and *trans*-bis(trifluoromethyl)dioxodiazine. Density functional theory (UB3LYP/6-311+G(2d)) was used to calculate the structure and vibrational spectrum of such a dimer.[18] Due to apparent diradical character in the dimer, it was necessary to mix HOMO and LUMO wave functions to achieve SCF stability.[19] Three distinct bound dimers (depicted in Figures 4−6) were found: *trans* and *cis* (both possessing C_2 symmetry) and a skewed (C_1) triplet. Ordinarily, one would expect the *trans* dimer to possess C_{2h} symmetry and the *cis* dimer C_{2v} symmetry, but the trifluoromethyl group orientations reduce the symmetry (slightly in the *trans* case, more significantly in the *cis*). All of these are predicted to have energies within 30 kJ mol^{-1} of the ground-state energies of the separated monomers, but only the *trans* dimer is predicted to be stable relative to the separated monomers. The low energy of the triplet dimer is reflective of the diradical nature of the dimers. The NN bonds range from 133.5 pm for the *trans* rotamer to 150.1 pm for the *cis* rotamer. The bond length for the skewed triplet is predicted to be 145.8 pm. These values are longer than those observed in

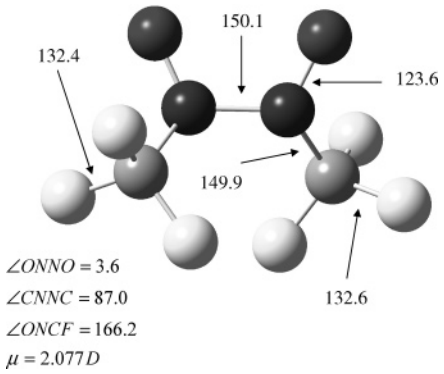

Figure 5. DFT structure of *cis*-bis(trifluoromethyl)dioxodiazine. Distances are given in picometers.

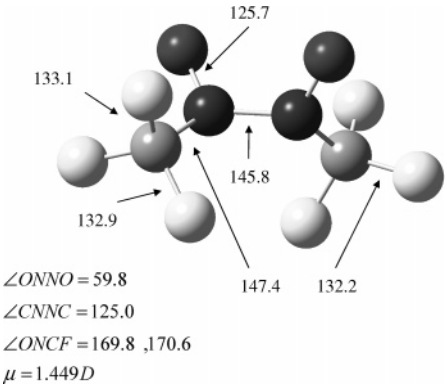

Figure 6. DFT structure of triplet bis(trifluoromethyl)dioxodiazine. Distances are given in picometers.

previously characterized nitroso dimers, such as $(CH_3NO)_2$. The harmonic vibrational frequencies for these dimers were calculated and scaled by a factor of 0.997, which was derived using the method of Scott and Radom[20] from comparison with the known matrix values for a selected group of compounds of interest in this study. A complete list of structural parameters and energies (electronic energy plus scaled zero-point energy) for the dimers and the ground and lowest triplet states for the monomer may be found in the Supporting Information. The scaled DFT vibrations and intensities for the dimers are presented in Table 2.

The Raman scattering activities (Table 2) were also calculated for the dimers. The *trans* dimer should exhibit intense scattering at 1512, 1024, and 783 cm^{-1} (due to the symmetric NO stretch, NN stretch, and symmetric CN stretch, respectively). The *cis* dimer should exhibit intense scattering at 1416 and 1403 cm^{-1} (due to the symmetric and asymmetric NO stretches, respectively). The triplet dimer should have only one vibration with appreciable Raman activity: that of the symmetric CN stretch at 758 cm^{-1}.

van der Waals Dimers. Optimized geometries for van der Waals dimers of the molecule were obtained (B3LYP/6-311+G(2d), without mixing): four singlets (two *trans* and two *cis*) within 2 kJ mol^{-1} of the separated monomers and three triplets (two *cis* and one skewed) within 2 kJ mol^{-1} of the separated $S_0 + T_1$ monomer pair. Counterpoise calculations indicate that the basis set superposition error may be on the order of 1.1−1.7 kJ mol^{-1} for the van der Waals species.[21] Structural parameters, vibrational frequencies, and energies for these may be found in the Supporting Information. The vibrational frequency shifts are predicted to occur, in most cases, within the line widths of our infrared features, and would not be observed in our spectra. The small binding energies predicted for these dimers indicate

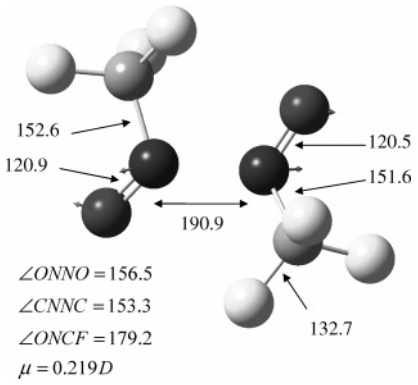

Figure 7. Transition species for *trans*-bis(trifluoromethyl)dioxodiazine. Distances are given in picometers. The displacement vectors represent the motions corresponding to the reaction coordinate.

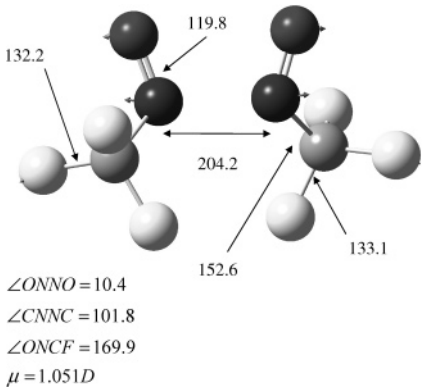

Figure 8. Transition species for *cis*-bis(trifluoromethyl)dioxodiazine. Distances are given in picometers. The displacement vectors represent the motions corresponding to the reaction coordinate.

that they would not be present in appreciable amounts in the gas phase, but arise in the matrix when neighboring matrix sites are occupied by the monomer.

Transition Species. Transition-state calculations[22] were carried out to determine the dimerization barrier for the three dimers. Vibrational calculations were performed for each of the predicted transition species. The structural parameters of the three transition species (depicted in Figures 7−9) may be found in the Supporting Information. It is noteworthy that the lowest energy transition species is that for the *cis* rotamer, 17.1 kJ mol^{-1} above the separated monomers and 6.5 kJ mol^{-1} above the *cis* dimer.

Excited States. Time-dependent DFT (UTD-B3LYP/6-311+G(2d))[23] studies were performed for each of the dimer species to determine the nature of the states to which the dimers were excited. For each dimer, the calculations predict a favorable transition (large oscillator strength) from the ground state (at its calculated geometry) to an excited state with a transition energy accessible in the UV. For the *cis* dimer, a transition is predicted to occur at 352 nm ($f = 0.046$), for the *trans* dimer at 292 nm ($f = 0.168$), and for the triplet at 269 nm ($f = 0.010$) and 207 nm ($f = 0.032$). Attempts to optimize (UCIS/6-31+G(d†))[24] the geometries of the excited states of the dimers were unsuccessful, with each optimization following an ever-increasing NN bond length, indicating that UV excitation of the dimers is to dissociative states, leading to monomer formation. The S_0-S_1 transition is only slightly shifted for the van der Waals dimers, and the oscillator strengths for these transitions are largely unaffected by complexation.

Figure 10 shows the energies (including scaled zero-point energies) of the various dimers and transition species relative

TABLE 2: DFT (B3LYP/6-311+G(2d)) Vibrational Frequencies (cm^{-1}) and Infrared (km mol^{-1}) and Raman ($Å^4$ amu^{-1}) Intensities for $(CF_3NO)_2$

	trans $(CF_3NO)_2$			*cis* $(CF_3NO)_2$			triplet $(CF_3NO)_2$		
vibration	ν	IR	Raman	ν	IR	Raman	ν	IR	Raman
NN stretch	1024	0	17	891	15	8	988	1	3
NO stretch	1512	0	19	1416	167	27	1368	34	6
NO stretch	1359	515	0	1403	3	13	1364	3	9
CF stretch	1271	371	0	1260	239	2	1252	62	1
CF stretch	1265	0	1	1231	532	1	1250	506	1
CF stretch	1233	644	0	1213	148	1	1206	505	2
CF stretch	1215	0	2	1207	352	0	1186	65	0
CF stretch	1118	0	2	1134	232	1	1159	35	0
CF stretch	1069	690	0	1125	350	4	1151	567	0
CN stretch	853	5	0	935	106	0	899	82	0
CN stretch	783	0	18	744	6	8	758	5	17
CF_3 deformation	723	0	3	729	83	1	716	101	0
CF_3 deformation	703	72	0	644	1	2	661	9	4
CF_3 deformation	601	2	0	624	12	2	635	1	3
CF_3 deformation	593	0	1	589	6	2	579	2	0
CF_3 deformation	541	12	0	557	3	2	572	7	0
CF_3 deformation	532	0	2	489	7	2	506	1	6
CNO bend	464	0	0	486	3	0	499	1	0
CNO bend	440	2	0	441	1	1	442	4	1
CNO bend	418	2	0	436	0	4	432	0	2
CNO bend	375	0	5	362	1	6	344	6	1
CF_3 rock	359	13	0	342	6	2	323	0	3
CF_3 rock	330	0	1	278	1	1	301	0	6
CF_3 rock	243	7	0	259	3	3	246	2	0
CF_3 rock	229	0	1	252	3	1	211	0	1
$ONCF_3$ rock	220	0	3	180	2	2	148	1	2
$ONCF_3$ rock	158	1	0	159	0	2	129	1	0
NN torsion	102	0	3	89	1	1	46	0	0
CF_3 torsion	61	0	0	24	0	0	35	0	0
CF_3 torsion	50	1	0	15	0	0	27	0	0

TABLE 3: Vibrational Assignment for $(CF_3NO)_2$

frequency (cm^{-1})					
Ar	Kr	Xe	N_2	O_2	assignment
	2846		2853	2858	2× (asymmetric NO stretch, *cis*)
1431	1426	1427	1431	1429	asymmetric NO stretch, *cis*
			1427		
1357	1357	1354	1359	1358	asymmetric NO stretch, *trans*
1302			1316		
1271	1267		1267	1268	CF stretch, *trans*
1264		1265			CF stretch, *cis*
1209					CF stretch, *cis*
1165					CF stretch, *cis*
1153	1145	1146	1150	1148	CF stretch, *cis*
1117	1112	1111	1114	1112	CF stretch, *cis*
1095	1091	1090	1094	1092	CF stretch, *trans*
977	982	976	980	981	asymmetric CN stretch, *cis*
		779			CC stretch, *cis*
746	746	745	747	750	CF_3 deformation, *cis*
				747	
709	709	709	709	709	CF_3 deformation, *trans*

to separated singlet and triplet monomers. Included in this figure are the energies of other possible species that may contribute to the observed spectra: CF_3, NO, and $(CF_3)_2NO$. Preliminary calculations indicate that the nitritoamine compounds are at much lower energies than the separated monomers. Structures for these may be found in ref 25.

Vibrational Assignment. The assignment of the visible photoproduct peaks may be found in Table 3. The observed features agree with those predicted in the DFT study. Furthermore, there is agreement among the predicted Raman features and those observed by Shurvell et al.[15] The 1515 cm^{-1} peak observed in their Raman studies may be assigned to the symmetric NO stretch of the *trans* dimer, which would have been formed as a result of the Raman source irradiation of the condensed monomer. The remaining Raman peaks (*trans*, *cis*, and triplet) will occur in regions that may be obscured by the parent compound's CF and CN stretches and CF_3 deformations. We predict no intense Raman feature at 1122 cm^{-1}, but two moderately intense peaks are expected at 1125 and 1118 cm^{-1} (*cis* and *trans*, respectively) in a region that is between observed monomer Raman peaks at 1172 and 1057 cm^{-1}. An additional unassigned and unreported Raman peak was observed (on the University of Queensland instrument[26]) at 1044 cm^{-1}, which may be assigned to the NN stretch of the *trans* dimer. The vibrations may be assigned to one or another of the singlet dimers; no peak unique to the triplet dimer was observed in any of the experiments.

Formation Efficiency. To elucidate the kinetics of the production of the visible photoproduct, the apparent quantum efficiency was determined as a function of irradiation time. The beam from the laser was broadened using a glass lens so that the entire matrix was irradiated evenly. The intensity (W cm^{-2}) of the radiation was determined using the laser power meter, which had been factory calibrated for use at 633 nm. These studies were performed in a dark laboratory, with the FTIR beam blocked whenever spectra were not being acquired, so that the incident radiation was the only source of photoproduct.

The apparent efficiency is a measure of the amount of visible photoproduct produced as a function of the amount of 633 nm light absorbed by the monomer. The gas-phase extinction coefficients, in combination with the infrared absorbance, were used to calculate visible absorbances. Thus

$$\Phi = \frac{\Delta A_{ir} a}{t \epsilon_{ir} I_0 (1 - 10^{-A_{ir}'(\epsilon_v/\epsilon_{ir})})} \quad (1)$$

becomes the equation used in these calculations, where A_{ir} is the infrared absorbance of the particular dimer band, a the area

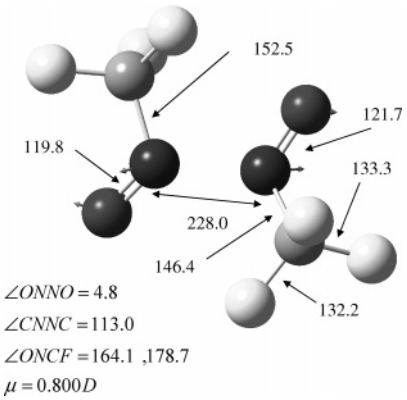

Figure 9. Transition species for triplet bis(trifluoromethyl)dioxodiazine. Distances are given in picometers. The displacement vectors represent the motions corresponding to the reaction coordinate.

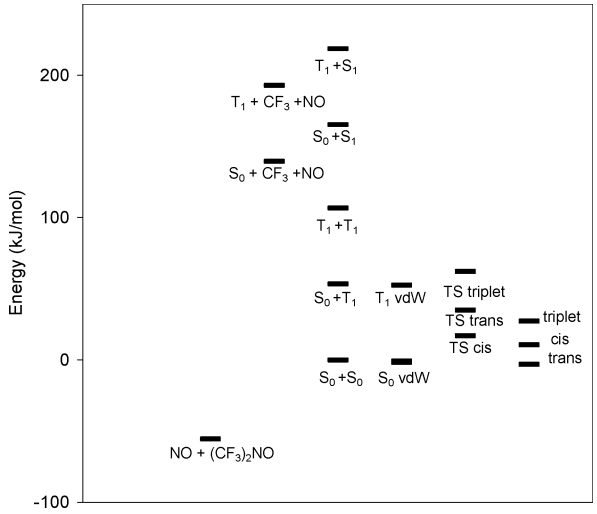

Figure 10. Energy level diagram for the $CF_3NO + CF_3NO$ system. The sum of the electronic and scaled zero-point energies was calculated for each species, and expressed relative to that of the separated ground-state monomers. The details of the calculations may be found in the text.

(cm^2) of the substrate window in the infrared beam, t the duration of the irradiation period (s), ϵ_{ir} the extinction coefficient for the particular infrared band ($cm^2\ mol^{-1}$), I_0 the intensity of the incident radiation (einsteins s^{-1}), A_ν the absorbance of the sample at the wavelength of irradiation, and A_{ir}' the absorbance of the monomer band. The extinction coefficients for the monomer were assumed to be identical to the gas-phase values, in both the visible[14] and infrared.[15] The derivation of this equation and the values for the monomer extinction coefficients may be found in ref 16. The extinction coefficients for each of the dimer bands (1357 and 1430 cm^{-1}) were determined by multiplying the 1595 cm^{-1} parent extinction coefficient by the ratio of the gain in product (1357 or 1430 cm^{-1}) absorbance to the loss of parent (1595 cm^{-1}) absorbance. Figure 11 depicts the behavior of the apparent quantum efficiencies in these experiments. The apparent efficiency begins at a low level and decreases over the course of the visible irradiation.

Discussion

Structures of the Dimers. The predicted NN stretch frequencies for the dimers (1024 and 891 cm^{-1} for *trans* and *cis*, respectively, 988 cm^{-1} for the triplet) are all well below the expected range. These indicate that the NN bond in each of these dimers is best described as a single bond. This implies

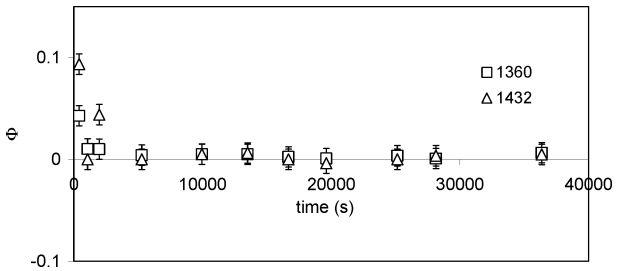

Figure 11. Apparent quantum efficiency (calculated using eq 1) for dimer formation in argon (CF_3NO:M = 1:30) as a function of irradiation time.

that these dimers have less π delocalization than is observed in the typical dimer, such as $(CH_3NO)_2$. Consequently, a greater degree of electron density is present in the NO bonds, which is reflected in a shortening of the NO bond to124−126 pm. Only one of the three dimers, the *trans* conformer, exhibits the planar symmetry common to most other nitroso dimers. The other two conformers, each with significant diradical character, are puckered at the nitrogen. The *cis* conformer has its NO bonds aligned, but the carbons are well out of the ONNO plane.

A measure of the propensity of nitroso compounds to dimerize has been found in the length of the NO bond in the monomer.[9,27] A convenient proxy for this has been the NO stretching frequency. Dimerization has been shown to occur for those molecules having NO stretching frequencies between 1480 and 1590 cm^{-1}, corresponding to bond lengths of 119.2−123.0 pm. The frequency for CF_3NO is just above the upper cutoff, and while the NO stretching frequency for the S_1 species was determined to be 1446 cm^{-1}, the bond length was determined to be 120 pm,[28] within the dimerization window on the bond length scale. DFT optimization of the triplet monomer yields a NO bond length of 122.1 pm, while a CIS optimization of the excited singlet state yields a length of 118.0 pm. Since the rationale for the use of the NO bond length in predicting dimerization comes from the sensitivity of the NO bond to the electron-withdrawing effects of the substituent, we see no reason to avoid a cautious extension of this rule to the excited-state surface.

An examination of the Mulliken charge distributions in the monomer and dimers yields some insight into the unusual nature of the dimerization of this molecule. The oxygen atoms in the *trans* dimer are 0.2 e^- more negative than they are in the monomer. Glaser et al. note identical levels of charge redistribution in their natural atomic charge calculations of the dimerization of CH_3NO.[2] We find this change to be less dramatic in the *cis* or triplet dimer, where the oxygen atoms each gain no more than 0.1 e^- of negative charge upon dimerization. A slight reduction in charge on the nitrogen atoms is noted for the *trans* dimer, less so for the *cis* and triplet. The nitrogen of the excited-state monomer is more negative than that of the ground state. This is to be expected given the n,π^* transition leading to the excited state. Thus, it may be that, to get sufficient charge at the nitrogen atoms to drive the dimerization, charge must first be withdrawn from the oxygen atoms via an electronic excitation. Of course, this is another way of saying that the highest occupied dimer orbitals correlate with unoccupied orbitals of the separated monomers.

Monomer Excited States. An electron energy loss spectroscopy (EELS) study by Walker places the lowest triplet state at 1.1 eV (106 kJ mol^{-1}).[29] The EEL spectrum probes the excited-state energy at the ground-state geometry, so the zero level energy of the triplet state will be lower than 106 kJ mol^{-1}, perhaps substantially so, given that the ground state is in an

eclipsed conformation, while the triplet is predicted to be in a staggered conformation, as is the first excited singlet state. The time-dependent DFT calculation for the monomer predicts the transition from the ground state to S_1 to occur at 691 nm, with an oscillator strength of 2×10^{-4}, in good agreement with the experimental values of Gordon and co-workers, who report the S_0-S_1 origin at 728 nm ($f = 2 \times 10^{-4}$),[28] and Dyet and co-workers, who report the origin at 718 nm.[30]

van der Waals Dimers. The van der Waals dimers predicted by the DFT calculations are all weakly bound, and their infrared spectra are expected to show little deviation from the monomer values. As a result, it should be difficult to locate IR evidence of van der Waals species in spectra of 1 cm^{-1} resolution in our relatively concentrated matrixes. Spectra acquired at higher resolution in dilute matrixes may yield evidence of these dimers. The "site effects" described by Clemitshaw and Sodeau (argon, R:M = 1:10000, 0.5 cm^{-1} resolution) may include one or more of these dimers.[13]

Formation of the Dimers. The energies of the transition species for the dimerization processes indicate that the dimerization should not occur spontaneously. For all three dimers, the dimerization pathway involves swings of as much as 20° in the ONNO dihedral angle. Large variations (sometimes uncoordinated) in the FCNO dihedral angle were also observed. Regular variation in the NO bond length was observed as the NN distance was decreased: the NO bond lengthens from 119 to 125 pm as the singlet dimers are formed. Once the dimerization threshold is crossed, the subunit geometries are coordinated. Similar effects are noted for the triplet dimerization. This is an example of a non-least-motion pathway, which has been shown to represent the mode of dimerization for nitrosomethane (CH_3NO).[31−33] It should be noted that the most stable dimer (*trans*) has the largest barrier to dimerization (37 kJ mol^{-1} difference between the van der Waals dimers and the transition species), while the *cis* (19 kJ mol^{-1}) and triplet (10 kJ mol^{-1}) dimers have smaller, though not negligible, barriers. The existence of a nonnegligible barrier to triplet dimerization also indicates that dimerization occurs on a surface at a higher level of excitation than $S_0 + T_1$. The low laser fluence in these experiments makes it unlikely that dimerization results from nearest neighbor monomers both excited simultaneously, or that a single monomer is doubly excited. One possible mechanism placing the molecules on one of these surfaces would be a collision-induced process

$$S_0 + S_0 \xrightarrow{h\nu} S_1 + S_0 \rightarrow T_1 + T_1 \rightarrow (CF_3NO)_2 \qquad (2)$$

which our DFT calculations (but not Walker's EELS data) predict to be energetically feasible.

The lack of features that can be assigned solely to the triplet dimer does not necessarily mean that the triplet is not being formed. It may be formed at a geometry for which one of the singlet surfaces provides a lower energy. Thus, the triplet dimer would be formed, but would relax to one of the singlet surfaces via intersystem crossing (ISC). A singlet calculation for the dimer at the triplet-optimized geometry yields a higher energy species, indicating that ISC should not occur from the minimum of the triplet surface. However, a singlet calculation performed at the geometry predicted for the triplet transition species yields an energy lower (by nearly 24 kJ mol^{-1}) than that of the triplet transition species. Thus, the possibility exists that any molecule formed on the triplet surface may relax to a singlet surface, presumably leading to the *cis* conformation, which more closely resembles the triplet geometry.

Other photoproduct structures could possibly satisfy the conditions imposed by the observed bands in the infrared spectra. A number of diazine compounds, including isomers of $F_3CO-N{=}N-OCF_3$, may be envisioned as possible stable products. DFT calculations do not predict peaks in the 1350−1430 cm^{-1} range for any of these. Furthermore, UV photolysis would not lead back to CF_3NO: rather F_2CO and N_2F_2 (or NF) would be the expected UV photoproducts. Another energetically feasible product would be the aforementioned $(CF_3)_2NONO$. This species also has an energy well below that of the separated monomers, yet is completely absent from any of the spectra, save those which were irradiated during deposition. This and the lack of other fragmentation products (CF_3, NO, $(CF_3)_2NO$, CF_2O, or FNO) lead us to conclude that the pathway is one which does not involve fragmentation as a first step. There has been no evidence of ground-state dimerization in any of the supersonic molecular beam studies of this molecule.[30,34,35]

The bis(trifluoromethyl) nitroxide ($(CF_3)_2NO$) radical is often found as the result of inadvertent ambient light photolysis of CF_3NO-containing samples.[36] The gas-phase infrared spectrum of this compound has been obtained by Blackley and Reinhard,[37] with peaks at 1395, 1290, 1230, 995, and 728 cm^{-1}. These peaks are close to those of the observed photoproducts, but assignment of the observed spectrum to the matrix-isolated radical would require a large matrix-induced shift that also is insensitive to the nature of the matrix material. While one may find reason to believe that the NO stretch may be sensitive enough to be shifted strongly by the matrix, this would lead to the expectation that the change in matrix from argon to xenon, krypton, nitrogen, and oxygen should also have a dramatic effect on the frequency of this vibration. We do not observe the NO (or $(NO)_2$) that would also appear as a result of the nitroxide formation. Blackley and Reinhard note that the radical dimerizes in $CFCl_3$ solution as the temperature is lowered, with an abrupt decrease in radical concentration and solidification of the solution at 113 K. They do not report an infrared spectrum of that dimer.

The gas-phase "dimerization" is initiated by the scission of the C−N bond in CF_3NO, resulting in NO and CF_3 fragments. These then react sequentially, with $(CF_3)_2NO$ as an intermediate, with an intact monomer unit to form $(CF_3)_2NONO$.[8] If the parent molecule leaves the excited state during the time required for fragmentation (measured in the gas phase to be 40 ns at 633 nm and 200 ns at 670 nm[34]), then this reaction will be quenched. In the previous matrix experiments, the dilution of the monomer was such that the nascent fragments recombined or remained isolated without a second monomer being found for reaction. In our more concentrated matrixes, there is a higher likelihood that an excited-state molecule will have a ground-state molecule in a neighboring lattice site, leading to the observed dimerization. The short-lifetime components in the fluorescence emission spectrum of matrix-isolated CF_3NO observed by Goodman and Brus[10] that result from annealing (to 22 K in N_2) or from elevated deposition temperatures (6−8 K in Ne (R:M = 1:2000)) may actually arise from the excited-state dimerization of the monomer and other radiationless processes involving monomer species inhabiting nearby matrix sites.

Additional kinetic information may be obtained by examining dimer formation in an oxygen matrix. The low-lying electronic states of O_2 would be expected to allow for the quenching of S_1 CF_3NO before it can react or fragment as the oxygen accepts the energy from CF_3NO^* in a time shorter than necessary for reaction or relaxation. However, no significant decrease in dimer formation is noted in the oxygen matrix. This indicates that the

rate constant for dimer production is comparable to the quenching constant for oxygen. While O_2 has been widely studied as a quenching agent, such studies have not been extended to CF_3NO, nor have quenching studies been extended to impurities trapped in rare gas or oxygen solids.

It is interesting that the rate of dimer formation appears to be maximized in the krypton matrixes. The fragmentation process in the gas phase has been shown to proceed through S_1-T_1 intersystem crossing (ISC) and S_1-S_0 internal conversion (IC),[30,35,38] with both processes showing sensitivity to the vibronic excitation level. The influence of the matrix gas may appear in the form of a vibrational relaxation process mediated by phonons in the matrix lattice or an external heavy atom effect mediating ISC, through a change in the vibronic coupling of the promoting mode for ISC or IC, or through a solvent-induced change in the visible absorptivity.

The effect of parent concentration on the dimer production is profound. The rate of dimer production is diminished in the dilute matrixes, as shown in Figure 2. The line in this figure represents a statistical description of the dimer production. The maximum observed rate was multiplied by the relative probability of a dopant molecule having another dopant molecule as a near neighbor in the lattice. The probability was determined by assuming that the dopant molecule occupies a matrix site consisting of the loss of one matrix atom (molecule) and its twelve neighbors. Clemitshaw and Sodeau[13] used this approach to determine the probability of isolation for a CF_3I dopant molecule in an argon matrix. Subtracting the probability of isolation from unity should then yield the probability of nearest neighbors:

$$P = 1 - (1 - 1/(\mathrm{MR}))^{122} \qquad (3)$$

where MR is the dilution ratio. This line represents only a crude statistical description, since the model assumes a perfect matrix crystal lattice, a reasonable assumption in Clemitshaw and Sodeau's dilute case, but hardly likely in these very concentrated matrixes. Also, the size of the matrix cage, and hence the number of nearest neighbor atoms (molecules), will vary with matrix gas, as the size of the atoms (molecules) and crystal structures vary. Nonetheless, the initial rates seem to follow the statistically predicted dependence on dilution. At the highest concentrations, many of the parent molecules will have at least one neighboring site occupied by another parent species. As the dilution increases, the likelihood of a neighboring site being occupied by another parent molecule decreases. The statistical description is also in agreement with the observed behavior of the apparent quantum efficiency for photoproduct production. In the experiment depicted in Figure 11, the initial apparent quantum efficiency is larger than the subsequent apparent quantum efficiencies: those monomers trapped in the most advantageous orientations for dimerization react rapidly, leaving behind those in less favorable configurations. Eventually the neighboring pairs are depleted altogether. The apparent quantum efficiency tapers off to much smaller values, limited by whatever migration might occur as isolated monomers, having been excited by the incoming radiation, donate energy to the surrounding lattice, providing some localized annealing. The apparent quantum efficiency is also much lower than the gas-phase value of approximately unity. The effect of laser flux on dimer production is approximately linear, leading us to conclude that only one parent molecule needs to be in its excited state for the dimerization to occur.

Conclusions

Trifluoronitrosomethane is the first example of a nitroso compound found to dimerize exclusively via electronic excitation. The postphotolysis infrared spectrum resembles that found for the visible photoproduct of the glassy liquid phase of CF_3NO. The observed vibrations correspond to *cis*- and *trans*-bis(trifluoromethyl)dioxodiazine. These vibrational assignments (infrared and glassy liquid Raman) are in agreement with the vibrational spectra predicted by DFT. The vibrational spectra are consistent with dimers possessing substantial diradical character and weak NN bonding. There is kinetic support for the formation of the dioxodiazine species in that there is a clear dependence on concentration, noted by the dramatic attenuation in dimer production with decreasing concentration. In the condensed phase, dimer production is contingent upon having a nearby monomer unit available for reaction with an excited molecule, all of which occurs in a time less than that required for fragmentation or relaxation of an excited CF_3NO molecule. The lack of production of any new species as a result of UV irradiation of the product indicates that no rearrangement of monomer connectivity occurs in the dimerization. Visible irradiation of the monomer in the condensed phase in relatively high concentration is required to promote the production of the dimer.

There are several aspects of the production of this dimer that warrant further study. Among these are more detailed kinetic studies and experiments designed to elaborate on the proposed structure (such as ESR, NMR, and Raman with a source wavelength exceeding 700 nm). An ESR examination of the matrix products could be used to indicate the presence of the triplet dimer with a greater sensitivity than that provided by IR: the DFT studies predict nitrogen hyperfine splitting (hfs) of 19 MHz and pairs of fluorine hfs of 20, 9, and −2 MHz.

Since the *trans* dimer is predicted to be stable relative to the separated monomers, we would expect it to remain as the matrix is warmed, and the possibility exists that it may be synthesized in bulk via 633 nm irradiation of the solid or glassy liquid.

Acknowledgment. Discussions with Professors Brian Gowenlock and Joan Mason were invaluable in the development of this paper. Spectra graciously provided by Professor H. F. Shurvell are gratefully acknowledged. Conversations with Professors Michael Cann and Norman Craig also proved useful in the development of this work. We appreciate the helpful comments of the reviewers. We acknowledge support from the donors of the Petroleum Research Fund, administered by the American Chemical Society (ACS-PRF Grants 17415-GB5 and 19904-B5), the National Science Foundation (Grant NSF-ILI USE-9250432), and the Faculty Research Committee of the University of Scranton.

Supporting Information Available: DFT electronic energies, bond lengths, bond angles, and zero-point energies for each of the monomers, dimers, and transition species, DFT vibrational frequencies and IR intensities for each singlet van der Waals dimer, and TD-DFT transition wavelengths and oscillator strengths for the monomer and singlet van der Waals dimers. This material is available free of charge via the Internet at http://pubs.acs.org.

References and Notes

(1) Gowenlock, B. G.; Lüttke, W. *Q. Rev.* **1958**, *12*, 321.
(2) Glaser, R.; Murmann, R. K.; Barnes, C. L. *J. Org. Chem.* **1996**, *61*, 1047.
(3) Haszeldine, R. N.; Jander, J. *J. Chem. Soc.* **1954**, 691.

(4) Jander, J.; Haszeldine, R. N. *J. Chem. Soc.* **1954**, 696.
(5) Haszeldine, R. N.; Mattinson, B. J. H. *J. Chem. Soc.* **1957**, 1741.
(6) Mason, J. *J. Chem. Soc.* **1963**, 4531.
(7) Mason, J. *J. Chem. Soc.* **1963**, 4537.
(8) Garmanov, A. B.; Vakhtin, A. B. *Int. J. Chem. Kinet.* **1996**, *28*, 71.
(9) Fletcher, D. A.; Gowenlock, B. G.; Orrell, K. G.; Sik, V.; Hibbs, D. E.; Hursthouse, M. B.; Malik, K. M. A. *J. Chem. Soc., Perkin Trans. 2* **1996**, 191.
(10) Goodman, J.; Brus, L. E. *J. Am. Chem. Soc.* **1978**, *100*, 2971.
(11) Bozlee, B. J.; Nibler, J. W. *J. Chem. Phys.* **1986**, *84*, 783.
(12) Demuth, R.; Burger, H.; Pawelke, G.; Willner, H. *Spectrochim. Acta, Part A* **1978**, *34A*, 113.
(13) Clemitshaw, K. C.; Sodeau, J. R. *J. Phys. Chem.* **1988**, *92*, 5491.
(14) Mason, J.; Dunderdale, J. *J. Chem. Soc.* **1956**, 754.
(15) Shurvell, H. F.; Dass, S. C.; Gordon, R. G. *Can. J. Chem.* **1974**, *52*, 3149.
(16) Giancarlo, L. C.; Haynie, B. C.; Miller, K. M.; Reynolds, J. M.; Rusnock, J. M.; Baumann, C. A. *J. Phys. Chem.* **1996**, *100*, 15539.
(17) Swanson, B. I.; Jones, L. H. *J. Mol. Spectrosc.* **1981**, *89*, 566.
(18) Frisch, M. J.; Trucks, G. W.; Schlegel, H. B.; Scuseria, G. E.; Robb, M. A.; Cheeseman, J. R.; Zakrzewski, V. G.; Montgomery, J. A., Jr.; Stratmann, R. E.; Burant, J. C.; Dapprich, S.; Millam, J. M.; Daniels, A. D.; Kudin, K. N.; Strain, M. C.; Farkas, O.; Tomasi, J.; Barone, V.; Cossi, M.; Cammi, R.; Mennucci, B.; Pomelli, C.; Adamo, C.; Clifford, S.; Ochterski, J.; Petersson, G. A.; Ayala, P. Y.; Cui, Q.; Morokuma, K.; Malick, D. K.; Rabuck, A. D.; Raghavachari, K.; Foresman, J. B.; Cioslowski, J.; Ortiz, J. V.; Baboul, A. G.; Stefanov, B. B.; Liu, G.; Liashenko, A.; Piskorz, P.; Komaromi, I.; Gomperts, R.; Martin, R. L.; Fox, D. J.; Keith, T.; Al-Laham, M. A.; Peng, C. Y.; Nanayakkara, A.; Gonzalez, C.; Challacombe, M.; Gill, P. M. W.; Johnson, B.; Chen, W.; Wong, M. W.; Andres, J. L.; Gonzalez, C.; Head-Gordon, M.; Replogle, E. S.; Pople, J. A. *Gaussian 98*, revision A.7; Gaussian, Inc.: Pittsburgh, PA, 1998. Becke, A. D. *J. Chem. Phys.* **1993**, *98*, 5648. Lee, C.; Yang, W.; Parr, R. G. *Phys. Rev. B* **1988**, *37*, 785.
(19) Foresman, J. B.; Frisch, A. *Exploring Chemistry with Electronic Structure Methods*, 2nd ed.; Gaussian, Inc.: Pittsburgh, PA, 1996; pp 34−6.
(20) Scott, A. P.; Radom, L. *J. Phys. Chem.* **1996**, *100*, 16502.
(21) Simon, S.; Duran, M.; Dannenberg, J. J. *J. Chem. Phys.* **1996**, *105*, 11024. Boys, S. F.; Bernardi, F. *Mol. Phys.* **1970**, *19*, 553.
(22) Peng, C.; Ayala, P. Y.; Schlegel, H. B.; Frisch, M. J. *J. Comput. Chem.* **1996**, *17*, 49. Peng, C.; Schlegel, H. B. *Isr. J. Chem.* **1994**, *33*, 449.
(23) Stratmann, R. E.; Scuseria, G. E.; Frisch, M. J. *J. Chem. Phys.* **1998**, *109*, 8218. Bauernschmitt, R.; Alrichs, R. *Chem. Phys. Lett.* **1996**, *256*, 454. Casida, M. E.; Jamorski, C.; Casida, K. C.; Salahub, D. R. *J. Chem. Phys.* **1998**, *108*, 4439.
(24) Foresman, J. B.; Head-Gordon, M.; Pople, J. A.; Frisch, M. J. *J. Phys. Chem.* **1992**, *96*, 135.
(25) Ang, H. G.; Klapdor, M. F.; Kwik, W. L.; Lee, Y. W.; Mack, H.-G.; Mootz, D.; Poll, W.; Oberhammer, H. *J. Am. Chem. Soc.* **1993**, *115*, 6929.
(26) Shurvell, H. F. Private communication.
(27) Cameron, M.; Gowenlock, B. G.; Vasapollo, G. *J. Organomet. Chem.* **1991**, *325*, 325.
(28) Gordon, R. D.; Dass, S. C.; Robins, J. R.; Shurvell, H. F.; Whitlock, R. F. *Can. J. Chem.* **1976**, *54*, 2658.
(29) Walker, I. C. *J. Chem. Soc., Faraday Trans.* **1991**, *87*, 2887.
(30) Dyet, J. A.; McCoustra, M. R. S.; Pfab, J. *J. Chem. Soc., Faraday Trans. 2* **1988**, *84*, 463.
(31) Hoffman, R.; Gleiter, R.; Mallory, F. B. *J. Am. Chem. Soc.* **1970**, *92*, 1460.
(32) Lüttke, W.; Skancke, P. N.; Traetteberg, M. *Theor. Chim. Acta* **1994**, *87*, 321.
(33) Heiberg, A. B. *Chem. Phys.* **1977**, *26*, 309; **1979**, *43*, 415.
(34) Asscher, M.; Haas, Y.; Roellig, M. P.; Houston, P. L. *J. Chem. Phys.* **1980**, *72*, 768.
(35) DeKoven, B. M.; Fung, K. H.; Levy, D. H.; Hoffland, L. D.; Spears, K. G. *J. Chem. Phys.* **1981**, *74*, 4755. Spears, K. G.; Hoffland, L. D. *J. Chem. Phys.* **1981**, *74*, 4765. Bower, R. D.; Jones, R. W.; Houston, P. L. *J. Chem. Phys.* **1983**, *79*, 2799.
(36) Chatgilialoglu, C.; Ingold, K. U. *J. Am. Chem. Soc.* **1981**, *103*, 4833 and references therein.
(37) Blackley, W. D.; Reinhard, R. R. *J. Am. Chem. Soc.* **1965**, *87*, 802.
(38) Spasov, J. S.; Cline, J. I. *J. Chem. Phys.* **1999**, *110*, 9568.